HHS Public Access

Author manuscript

Int J Pharm. Author manuscript; available in PMC 2019 September 05.

Published in final edited form as:

Int J Pharm. 2018 September 05; 548(1): 443–453. doi:10.1016/j.ijpharm.2018.07.010.

Composite particle formulations of colistin and meropenem with improved *in-vitro* bacterial killing and aerosolization for inhalation

Sharad Mangal[1], **Heejun Park**[1], **Lingfei Zeng**[1], **Heidi H. Yu**[2], **Yu-wei Lin**[2], **Tony Velkov**[3], **John A. Denman**[4], **Dmitry Zemlyanov**[5], **Jian Li**[2], and **Qi (Tony) Zhou**[1,*]

[1]Department of Industrial and Physical Pharmacy, College of Pharmacy, Purdue University, 575 Stadium Mall Drive, West Lafayette, IN 47907, USA

[2]Monash Biomedicine Discovery Institute, Department of Microbiology, Monash University, Clayton, Victoria 3800, Australia

[3]Department of Pharmacology & Therapeutics, Faculty of Medicine, Dentistry and Health Sciences, The University of Melbourne, Parkville, Victoria 3010, Australia

[4]Future Industries Institute, University of South Australia, Mawson Lakes, SA 5095, Australia

[5]Birck Nanotechnology Center, Purdue University, West Lafayette, IN 47907, USA

Abstract

Antibiotic combination therapy is promising for the treatment of lower respiratory tract infections caused by multi-drug resistant Gram-negative pathogens. Inhaled antibiotic therapy offers the advantage of direct delivery of the drugs to the site of infection, as compared to the parenteral administrations. In this study, we developed composite particle formulations of colistin and meropenem. The formulations were characterized for particle size, morphology, specific surface area, surface chemical composition, *in-vitro* aerosolization performance and *in-vitro* antibacterial activity. The combinations demonstrated enhanced antibacterial activity against clinical isolates of *Acinetobacter baumannii* N16870 and *Pseudomonas aeruginosa* 19147, when compared with antibiotic monotherapy. Spray-dried meropenem alone showed a poor aerosolization performance as indicated by a low fine particle fraction (FPF) of 32.5 ± 3.3%. Co-spraying with colistin improved the aerosolization of meropenem with up to a two-fold increase in the FPF. Such improvements in aerosolization can be attributed to the enrichment of colistin on the surface of composite particles as indicated by X-ray photoelectron spectroscopy (XPS) and time-of-flight secondary ion mass spectrometry (ToF-SIMS), and the increases in particle porosity. Intermolecular interactions between colistin and meropenem were observed for the combination formulations as measured by FT-IR. In conclusion, our results show that co-spray drying with colistin improves the antibacterial activity and aerosol performance of meropenem and produces a formulation with synergistic bacterial killing.

*Corresponding Author: Qi (Tony) Zhou, Tel.: +1 765 496 0707, Fax: +1 765 494 6545, tonyzhou@purdue.edu.

Graphic Abstract

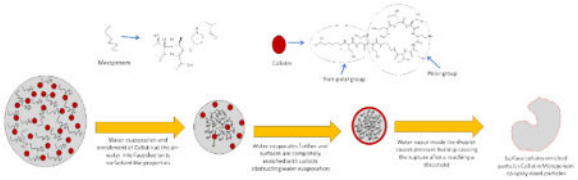

Keywords

Dry powder inhaler; aerosol performance; spray drying; antimicrobial synergy; meropenem; colistin

Introduction

Lower respiratory tract infections (or lung infections) cause high mortality and morbidity (Liang et al., 2011; Mizgerd, 2006; WHO, May 2014). Antibiotics administered *via* systemic routes are often not effective for lung infections, as for many antibiotics such as the polymyxins (polymyxin B and colistin) only a small fraction of the drug is available at the sites of infection (i.e. in the lungs) (Velkov, Abdul Rahim, Zhou, Chan, & Li, 2015). Simply increasing parenteral dose often causes severe systemic adverse effects (Traini & Young, 2009). For instance, high-dose parenteral colistin can lead to neurotoxicity and nephrotoxicity (Garonzik et al., 2011).

Colistin is often used for treatment of respiratory infections caused by multidrug-resistant (MDR) Gram-negative bacteria (Levin et al., 1999; Velkov et al., 2015). Recently, there is a marked increase in the incidence of colistin-resistant infections (Cai, Chai, Wang, Liang, & Bai, 2012; Marchaim et al., 2011; Paterson & Harris, 2016). Due to the dry development pipeline of novel antibiotics, combination therapy can be a practical and swift approach for treating the infections caused by colistin-resistant pathogens (Cai et al., 2012). However, synergistic antibacterial effects of systemically administered combination antibiotics can be compromised due to the different pharmacokinetic profiles (Weers, 2015), which may not allow both drugs to attain effective drug concentrations at the same time at the infection sites.

Antimicrobial therapy via the inhalation route has attracted increasing attentions for the treatment of lower respiratory infections (Velkov et al., 2015; Q. Zhou et al., 2015). Inhalation therapy substantially improves drug concentration on the airway surfaces with much reduced systemic exposure, hence maximizes the treatment efficacy and reduces the systemic toxicities (Cipolla & Chan, 2013; Montgomery, Vallance, Abuan, Tservistas, & Davies, 2014; Yapa et al., 2013). Additionally, inhalation therapy may be able to deliver combinational antibiotics to the same targeted infection sites simultaneously allowing greater opportunity to achieve intended synergistic effects. In addition, dry powder inhalers (DPIs) may enable the delivery of high-doses of antibiotics directly to the respiratory tracts (Q. Zhou et al., 2015).

Typically, the inhaled drug particles produced by traditional jet-milling approach are highly cohesive and have poor flowability and poor aerosolization performance (Y. W. Lin, Wong, Qu, Chan, & Zhou, 2015). Addition of excipients such as fine lactose particles may improve the aerosolization of cohesive powders to some extent (de Boer, Chan, & Price, 2012; Grasmeijer et al., 2014; Smyth & Hickey, 2005). However, for high-dose drugs like antibiotics, addition of excipients may increase the inhalation powder mass that needs an excessive number of inhalations to complete the dose and a bulky inhaler to accommodate the large dose (Q. Zhou et al., 2015).

Our earlier studies have indicated that the spray dried colistin particles without any excipient had high aerosol performance with fine particle fraction (FPF) > 80% with an Aerolizer® device (Q. Zhou et al., 2013). It was proposed that such high aerosol performance of the spray dried colistin powders is attributed to its surfactant-like properties (Mestres, Alsina, Busquets, Murányi, & Reig, 1998; Wallace et al., 2010), which allows self-assembly of non-polar tail at the air-liquid interface during spray drying resulting in the formation of low surface energy particles (Jong, Li, Morton, Zhou, & Larson, 2016). Previous studies have shown that surface-active components could also potentially self-assemble on the surface, when co-sprayed with a secondary component altering its surface physico-chemical and aerosolization properties (N. Y. Chew et al., 2005; Momin, Tucker, Doyle, Denman, & Das, 2018; Momin, Tucker, Doyle, Denman, Sinha, et al., 2018; Rabbani & Seville, 2005; Sou et al., 2013; Q. T. Zhou et al., 2016). The aim of this study was to investigate the effect of colistin on the aerosol performance of the co-spray dried formulations in synergistic combination with meropenem (Lenhard et al., 2016).

In this study, colistin was co-spray dried with meropenem to develop combinational DPI formulations. The resultant DPI formulations were characterized regarding particle size, morphology, surface chemical composition and specific surface area. The *in-vitro* aerosol performance and *in-vitro* antibacterial activity were characterized.

Materials and Methods

Materials

Colistin sulphate and meropenem trihydrate were purchased from ßetaPharma® (Shanghai) Co., Ltd (Wujiang City, JiangSu Province, China). Acetonitrile (HPLC grade) and sodium sulfate were purchased from Fisher Scientific (Fair Lawn, New Jersey, USA). Tryptone soy broth and Mueller-Hinton Broth were supplied by Oxoid Ltd, Basingstoke, UK and glycerol by Astral Scientific Pty Ltd, Taren Point, Australia.

Time– kill assays

Clinical isolates of *A. baumannii* N16870 and *Pseudomonas aeruginosa* 19147 were stored in tryptone soy broth with 20% glycerol at -80 °C and sub-cultured onto nutrient agar plates before each experiment. Time-kill studies were conducted for meropenem, colistin and combinations (Colistin:Meropenem_1:3, Colistin:Meropenem_1:1 and Colistin:Meropenem_3:1) against *A. baumannii* N16870 *and P. aeruginosa* 19147. All samples were dissolved in broth and experiments were performed with an initial inoculum of

~10^6 CFU/mL in 20 mL of Cation-Adjusted Mueller-Hinton Broth (CAMHB) in 50 mL pyrogen-free and sterile polypropylene tubes. Serial samples (50 μL) were collected at 0, 1, 2, 4, and 24 h for viable counting on nutrient agar plates and the limit of detection was 20 CFU/mL. A ProtoCOL automated colony counter (Synbiosis, Cambridge, United Kingdom) was used to quantify bacteria after 24 h of incubation at 37 °C. Bacterial growth was measured after 0, 1, 2, 4 and 24 h of incubation at 37 °C. A growth control without antibiotic was also tested.

Spray drying

A Büchi 290 spray dryer (Büchi Labortechnik AG, Falwil, Switzerland) was employed to produce the composite particles at the following parameters: inlet temperature 110 °C; outlet temperature 63 °C; aspirator 35 m^3/h; atomizer setting 700 L/h; feed rate 2 mL/min. The total solid content of the feed solutions was 13.3 mg/mL for all formulations. The feed solutions for the composite formulations were prepared by dissolving colistin and meropenem at the mass ratios of 3:1, 1:1 and 1:3 in water. The spray-dried samples were stored in a desiccator with silica gel at 20 ± 3 °C.

Scanning electron microscopy (SEM)

Samples were visualized using a scanning electron microscope (NOVA nanoSEM, FEI Company, Hillsboro, Oregon, USA). Adhesive carbon tapes were put on the stainless steel stub and then the formulations were scattered over the tape. A thin film of platinum was coated on the stubs using a sputter coater (208 HR, Cressington Sputter Coater, England, UK). The images were captured using the built-in software.

Particle size distribution

Image analysis based on SEM micrographs was used for particle sizing (Shekunov, Chattopadhyay, Tong, & Chow, 2007; Wan et al., 2013). Martin's diameter was measured as the indicator of physical particle size (n = 100) and D_{10}, D_{50} and D_{90} were calculated.

Powder X-ray diffraction (P-XRD)

Powder X-ray diffraction (Rigaku Americas, Texas, USA) was applied to evaluate crystallinity of the powders. Each powder formulation was spread on a glass slide and the XRD patterns were obtained from 5 to 40° 2θ at 5°/min.

Specific surface area and pore volume

Surface area and pore volume were measured using a TriStar3000 BET equipment (Micromeritics Instrument Company, Norcross, GA). Approximately 300 mg of each sample was filled into a BET sample tube and degassed overnight. Nitrogen with high purity was used as the adsorbate, and the adsorption behavior at varying relative pressure conditions was measured. The specific surface areas and pore volume of three replicates were determined.

Time-of-flight secondary ion mass spectrometry (ToF-SIMS)

Surface composition of the composite formulations was characterized using Time-of-flight secondary ion mass spectrometry (nanoToF instrument, Physical Electronics Inc., Chanhassen, Minnesota, USA) as described elsewhere with slight modifications (Q. Zhou et al., 2011). Data were obtained from 4 areas (100 × 100 μm each) per sample. Characteristic peak fragments for azithromycin and L-leucine were identified. For colistin, the peaks at m/z ~30 atomic mass unit (amu) and ~86 amu, corresponding to $[CH_4N^+]$ and $[C_5H_{12}N^+]$ fragments, respectively, were selected. For meropenem, the fragment at m/z ~ 68 amu corresponding to $[C_4H_6N^+]$ was selected as the characteristic peak. Sample spectra were processed using the WincadenceN software (Physical Electronics Inc., Chanhassen, MN, USA) to construct high-resolution surface composition maps.

X-ray photoelectron spectroscopy (XPS)

The surface composition of the composite formulations was evaluated quantitatively using X-ray photoelectron spectroscopy (XPS) (AXIS Ultra DLD spectrometer, Kratos Analytical Inc., Manchester, UK). The detailed XPS method was described previously (Mangal et al., 2015). A CasaXPS software (version 2313 Dev64) was applied to process the XPS data. Curve-fitting was performed following a Shirley background subtraction using model peaks obtained from pure compounds. The atomic concentrations of the elements in the near-surface region were estimated after a Shirley background subtraction taking into account the corresponding Scofield atomic sensitivity factors and inelastic mean free path (IMFP) of photoelectrons using standard procedures in the CasaXPS software assuming homogeneous mixture of the elements within the information depth (~10 nm).

Fourier transform infrared spectroscopy (FTIR)

The spray-dried powders were analyzed using an FTIR with attenuated total reflectance (ATR) (Cary 600 series FTIR spectrometer, Agilent Technologies, Santa Clara, CA, USA). A small amount of powder was carefully placed onto the ATR crystal, and the pressure disk was used to improve the uniformity of contact between the sample and the ATR crystal of the instrument. Samples were analysed at a resolution of 4 cm^{-1}. A background scan was collected initially, and the sample spectrum was collected subsequently with the built-in software automatically subtracting the background.

In-vitro aerosol performance

A Multi-Stage Liquid Impinger (MSLI) (Copley Scientific Limited, Nottingham, UK) was used to evaluate *in-vitro* aerosol performance with a USP induction port (USP throat). Each sample (10 ± 2 mg) was loaded into a capsule (size 3 hydroxypropyl methylcellulose capsules, Qualicaps, Whitsett, North Carolina, USA) and aerosolized by an RS01 DPI device (with a similar design to Osmohaler™, Plastiape S.p.A., Osnago, Italy). Aerosol performance of the formulations was tested using a standard dispersion procedure: 4 L of air was drawn to pass the inhaler at an airflow of 100 L/min for 2.4 s, with a pressure drop of ~4 kPa across the device (Mangal et al., 2018). Under these experimental conditions, the cutoff diameters for Stages 1, 2, 3 and 4 of MSLI were 10.4, 4.9, 2.4, and 1.2 μm, respectively. For Stages 1–4, water (20 mL) was filled in each stage prior to each aerosolization. Drug

retained in capsule, device, USP throat, Stages 1 – 4 and filter paper were dissolved in water and quantified. Emitted dose (ED) was defined as the collected drug except for those retained in the capsule and device, over the total recovered drug. Fine particle fraction (FPF) represents the fraction of the drugs deposited on Stage 3, Stage 4 and filter paper over the recovered dose (recoveries are in the range of 85 – 115% of the loaded doses). FPF-Emitted was calculated as the FPF over emitted dose.

Drug Quantification

Concentrations of colistin sulfate and meropenem were determined using a validated HPLC method. Briefly, the HPLC system with a C18 separation column (5 μm, 150 × 4.60 mm, Agilant, Waldbronn, Germany) was used (Shetty et al., 2018). The mobile phase consisted of 30 mM sodium sulfate (adjusted to pH 2.5 with H_3PO_4) (A) and acetonitrile (B). The isocratic elution program used for colistin and meropenem detection was 76% A and 24% B v/v for 7 min at the flow rate of 1.0 mL/min. The absorbance profile of both colistin and meropenem was monitored at 214 nm. Calibration curves prepared for colistin (0.0125 – 0.5 mg/mL) and meropenem (0.0125 – 0.5 mg/mL) in water were linear ($r^2 > 0.999$).

Statistical analysis

One-way analysis of variance (ANOVA) with the Tukey–Kramer post-hoc test was employed for statistical analysis using a GraphPad Prism software (GraphPad Software, Inc., La Jolla, CA, USA). The asterisks denote the statistical differences of groups as indicated on figures as *$p < 0.05$, **$p < 0.01$, ***$p < 0.001$, ****$p < 0.0001$ and NS for not significant ($p > 0.05$).

Results

Time kill assay

Figure 1 shows the time-kill profiles against clinical isolates of *A. baumannii* N16870 and *P. aeruginosa* 19147. For *A. baumannii* N16870, meropenem showed no antibacterial effect at 16 mg/L in 24 h, and marginal antibacterial activity at 48 mg/L in 2 h, albeit regrowth was observed in 4 h (Figure 1A). Colistin showed bacterial killing at both 16 and 48 mg/L; but at 16 mg/L regrowth was evident in 4 h. The combination of Colistin:Meropenem_1:1 (16:16 mg/L) demonstrated superior antibacterial activity than monotherapy with each drug. Colistin:Meropenem_1:3 (16 and 48 mg/L) and Colistin:Meropenem_3:1 (48 and 16 mg/L) showed more rapid killing kinetics than meropenem or colistin alone. It is noteworthy that all three combinations demonstrated eradication of the bacteria without any regrowth.

The antibacterial activity of the colistin and meropenem appeared to be weaker against *P. aeruginosa* 19147 (Figure 1B), even at a much higher concentrations (e.g. 192 mg/L), complete killing could not be achieved by either colistin or meropenem monotherapy at 24 h. The combination of Colistin:Meropenem_1:1 (64:64 mg/L) and Colistin:Meropenem_1:3 (64:192 mg/L) also did not achieve a complete bacterial killing after 24 h. A complete bacterial killing was observed only with the Colistin:Meropenem_3:1 (192:64 mg/L). These data show the difficulty in eradication of colistin-resistant strains of *A. baumannii* and *P. aeruginosa*. This is in agreement with previous studies indicating the antibacterial synergy

between meropenem and colistin against multi-drug resistance pathogens (Liang et al., 2011; Timurkaynak et al., 2006).

Scanning electron microscopy (SEM)

SEM images showed that the spray-dried meropenem particles are near-spherical with rough surfaces (Figure 2A); while the spray-dried colistin particles showed a mixed population of rough and smooth (hollow) particles as indicated by red arrows (Figure 2E). Morphology of the co-spray dried formulations changed substantially with varying colistin concentrations. Colistin:Meropenem_1:3 showed more proportion of rough particles (Figure 2B) than Colistin:Meropenem_1:1 (Figure 2D). The population of hollow and smooth particles appeared to increase with increasing feed colistin concentrations (as shown by red arrows). Some flake-shaped smooth particles are the fragments of shattered hollow particles.

Particle size distribution

Particle sizes of the spray-dried formulations are presented in Table 1. The results indicated that the D_{50} of spray-dried formulations was < 2 μm and D_{90} was < 3 μm. Therefore, the majority of particles were within the physical size range of 0.5 – 3 μm with no significant differences among formulations.

Specific surface area and pore volume

Table 2 shows the specific surface area and pore volume of the selected spray-dried formulations. The surface area and pore volume increased substantially with increasing the colistin feed concentration. The increase in surface area is likely attributed to the formation of porous particles, which have larger surface area than the non-porous particles.

Time-of-flight secondary ion mass spectrometry (ToF-SIMS)

To-SIMS images of the spray-dried formulations clearly showed that the surface composition changed substantially with varying colistin concentration (Figure 3). Colistin:Meropenem_1:3 particles showed an abundance of both colistin and meropenem on the surfaces (Figure 3B). The abundance of colistin on the particle surface was increased with an increase in colistin ratio in the combination formulations. It was noted that colistin dominated the particles surfaces in the Colistin:Meropenem_3:1 formulation (Figure 3D).

X-ray photoelectron spectroscopy (XPS)

Previous studies have suggested that surfactant-like molecules attains higher surface concentration due to their self-assembly at the air-water interface early in drying phase (Vehring, 2008; Vehring, Foss, & Lechuga-Ballesteros, 2007). Since colistin exhibits surfactant-like properties (Wallace et al., 2010), we also compared colistin and meropenem composition at the surface of selected formulations by XPS (Table 4). In agreement with the ToF-SIMS data, the XPS results also demonstrated that the surface concentration of colistin increased with an increase in colistin feed concentration (Table 3). The surface concentration of colistin was 46.8 % for the Colistin:Meropenem_1:3, which increased markedly to 67.6% and 87.7% for Colistin:Meropenem_1:1 and Colistin:Meropenem_3:1, respectively. Consistent with our hypothesis, colistin achieved higher surface concentration compared

with the theoretical value (where a homogeneous distribution of colistin and meropenem is assumed on the particle surfaces), suggesting enrichment of colistin on the surface of the spray dried particles.

We also investigated the relationship between colistin surface composition and specific surface area/pore volume as obtained by BET (Figure 3). The graph clearly shows that the surface area and pore volume increased with increasing surface colistin composition. The formation of porous particles may be attributed to the enrichment of colistin at the surface of the composite particles. We propose that the self-assembly of colistin at the air-water interface creates an environment to hinder the escape of water vapour from the bulk of the droplet leading to an increased vapour pressure. An increase in vapour pressure results in expansion of the colistin-rich interface and eventual burst of particles leading to formation of porous/ruptured particles. The observation that porosity and surface area increased linearly with increasing surface concentration suggests that surface concentration governs the degree of resistance to the escape of water vapor, where a higher concentration results in higher resistance intensifying particle rupture leading to the formation of more porous particles with higher surface area.

Fourier transform infrared spectroscopy (FTIR)

Potential molecular interactions between colistin and meropenem in the formulations were investigated by FTIR (Figure 5 and Table 4). Distinguishable characteristic FTIR peaks identified for the spray-dried colistin were at 1645.0 cm^{-1} (characteristic of the amide I C=O stretching), at 1525.4 cm^{-1} (characteristic of the amide II N-H bending) and at 1068.4 cm^{-1} (characteristic of stretching vibrations related to C-N) (Freudenthal et al., 2016). For the spray-dried meropenem, the stretching vibration peak of O-H in carboxylic acid group was observed at 2965.9 cm^{-1} (Abdelkader et al., 2017). The distinguishable peaks from the stretching vibrations of the C=O in the carboxyl group and β-lactam ring were observed at 1658.5 and 1756.8 cm^{-1}, respectively. The stretching vibrations of the C-N bond in the pyrrolidine ring, β-lactam ring and dimethylcarbamoyl group were observed at 1145.5, 1253.5 and 1373.1 cm^{-1}, respectively. In addition, the wagging and twisting vibrations of the C–H bonds in the hydroxyethyl substituent and the β-lactam ring were observed at around 1070 cm^{-1} (Cielecka-Piontek et al., 2013).

In the co-spray dried 1:1 mixture of meropenem and colistin, there were significant changes in the IR spectra compared to each spray dried pure component. The meropenem peaks that correspond to the stretching vibrations of O-H and C=O in the carboxyl group were shifted to lower wavenumbers of 2958.2 and 1650.8 cm^{-1}, respectively. In addition, the C-N stretching vibrations in the pyrrolidine ring and dimethylcarbamoyl group were shifted to 1139.7 and 1380.8 cm^{-1}, respectively. The multiple peaks of wagging and twisting vibrations of the C–H in the hydroxyethyl substituent and the β-lactam ring disappeared. In contrast, there were no significant change in the stretching vibrations peaks of C=O and C-N in the β-lactam ring. The peaks of colistin that correspond to the stretching vibrations of amide I C=O stretching and amide II N-H bending were shifted to the higher wavenumbers of 1650.8 and 1531.2 cm^{-1}, respectively. In addition, the C-N stretching vibrations were shifted to a higher wave number of 1074.1 cm^{-1}.

Powder X-ray diffraction (PXRD)

Raw meropenem was crystalline as evident by the sharp diffraction peaks (Figure 6). PXRD patterns indicated that both the raw and spray-dried colistin were amorphous (Q. Zhou et al., 2013). Meropenem was transformed from crystalline form to amorphous form after spray drying, which is attributed to rapid drying that leads to random orientation of meropenem molecules in the dried phase (Singh & Van den Mooter, 2016). Furthermore, the spray-dried combination formulations also showed no sharp peaks indicating that they are all amorphous and the phase separation on the particle surface as indicated by XPS was not a consequence of crystallization as noted in an earlier study (Feng et al., 2011).

In-vitro aerosol performance

In-vitro aerosol performance indicated by FPF and ED of the spray-dried powders are shown in Figure 7. The results show that the spray-dried meropenem had a relative low FPF of 32.4 ± 3.3 % indicating poor aerosolization performance (Figure 7A). All the combination formulations showed a substantially higher FPF than the spray-dried meropenem ($p < 0.0001$). Colistin:Meropenem_1:1 and Colistin:Meropenem_3:1 had the similar high FPF to the spray dried pure colistin formulation, which were more than two-fold of that for the spray-dried meropenem. Further increase in the colistin feed concentration from Colistin:Meropenem_1:1 to Colistin:Meropenem_3:1 had no significant effects in FPF. Furthermore, the ED of Meropenem-SD was as low as 47.3 ± 4.3 %, which was substantially lower than the spray dried colistin and the composite formulations ($p < 0.0001$). For FPF-Emitted, there is no significant difference between Meropenem-SD and Colistin:Meropenem_1:3; however, the FPF-Emitted values of Colistin:Meropenem_1:1 and Colistin:Meropenem_3:1 are significant higher than that of Meropenem-SD (Figure 7C). Moreover, colistin and meropenem had identical FPF or aerosol performance in each composite formulation.

Discussion

Combination antibiotic therapies are increasingly used to combat MDR Gram-negative lung infections (Mouton, 1999). This has spurred the search for effective colistin combinations that exhibit greater bacterial killing, improved safety and superior pharmacokinetics (Biswas, Brunel, Dubus, Reynaud-Gaubert, & Rolain, 2012; Q. Zhou et al., 2014; Q. T. Zhou et al., 2016). Typically, the antibiotics with different mechanisms of action can act synergistically to greatly enhance antibacterial killing. Colistin is a lipopeptide antibiotic that primarily acts by disrupting the outer membrane ultrastructure of Gram-negative bacteria leading to cell death (Velkov et al., 2013). Whereas meropenem is a carbapenem antibiotic which acts by binding to penicillin-binding proteins involved in the peptidoglycan formation and thereby compromises bacterial cell integrity (Davies, Shang, Bush, & Flamm, 2008; Kitzis, Acar, & Gutmann, 1989). Previous studies have shown that the combination of colistin (or polymyxin B) and meropenem exhibit synergistic anti-bacterial activity (Lenhard et al., 2016; Timurkaynak et al., 2006). Furthermore, colistin and meropenem combination therapy has been shown to be effective in the treatment of lung infections caused by MDR (Herrmann et al.).

Our time–kill results against the clinical isolate *A. baumannii* N16870 and *P. aeruginosa* 19147 demonstrated that colistin and meropenem monotherapy had weak antibacterial activity with considerable bacterial regrowth (except for *A. baumannii* N16870 treated with colistin at 48 mg/L). The combinations exhibited excellent antibacterial activity against *A. baumannii* N16870. In the case of *P. aeruginosa* 19147, complete bacterial killing was achieved with Colistin:Meropenem_3:1 (192:64 mg/L). This indicates that high local concentrations of antibiotics are required to achieve effective bacterial killing for certain Gram-negative species. However, in most cases such high concentrations of antibiotics in airway surfaces deep in the lungs cannot be achieve by systemic administrations (Garonzik et al., 2011). The inhalation route offers direct access of the drug to the lung surfaces and hence may be more suitable for treating respiratory tract infections caused by MDR Gram-negative bacteria “superbugs” (Velkov et al., 2015; Q. Zhou et al., 2015). In this study, for the first time we developed and characterized colistin and meropenem co-sprayed DPI formulations for the treatment of lower respiratory tract infections.

The spray dried colistin alone particles have two types of shapes: (i) smooth (some buckling) and hollow particles (ii) corrugated particles, which are in agreement with previous studies (Jong et al., 2016). It seems lower inlet temperatures (e.g. 80 °C) resulted in more particles with corrugated morphology (Zhou et al., 2013); while higher inlet temperature led to more hollow particles with smooth surfaces as shown in this study. This can be attributed to surfactant-like properties of colistin (Wallace et al., 2010). When drying temperature is high, a shell of colistin is formed on the interface, and solutes cannot diffuse towards the core due to rapid drying (Q. Vehring, 2008). In the drying process, wrinkled particles are formed because of initial high internal pressures due to solvent evaporation and then a decreased internal pressure leads to collapse of the shells. Some hollow particles are buckling because low colistin concentration leads to thin shell and high internal pressure causes rapture of the shell. This explains well that a higher drying temperature leads to more cenospheres or buckling particles attributed to more rapid evaporation of the solvent and higher internal pressure.

It is noted that colistin was more enriched on the particle surface than meropenem as shown by XPS data (Table 3). Meropenem has relatively lower water solubility (approximately 16.4 mg/mL) (Choi et al., 2012), and usually less water soluble component can accumulate on the particle surfaces during drying as the compound with lower solubility will reach supersaturation and precipitate quicker on the surface than the compound with higher solubility (Vehring et al., 2007). However, surfactant-like molecules such as colistin can self-assemble at the air-water interface (Lawrence, Alpar, McAllister, & Brown, 1993; Mestres et al., 1998; Wallace et al., 2010) leading to shell formation (Mangal et al., 2015; Mangal et al., 2016). Spray-dried colistin particles exhibits a lower surface energy than the jet-milled colistin (Jong et al., 2016), attributed to the self-assembly of colistin at the air water interface with a specific orientation with low energy hydrophobic tail facing outwards (Jong et al., 2016). Despite its lower aqueous solubility, meropenem did not enrich at the surface indicating that interfacial activity may be the dominant factor governing the surface enrichment in composite spray-dried formulations, which warrants further investigation.

The shell forming ability of colistin may alter the morphology, porosity and surface area of co-sprayed formulations, and therefore affects the aerosolization (N. Y. Chew & Chan, 2002; N. Y. K. Chew & Chan, 2001; N. Y. K. Chew, Tang, Chan, & Raper, 2005; Edwards et al., 2005). Our results clearly showed strong correlations between surface colistin concentration, surface area and porosity of the composite formulations (Figure 4), indicating that surface colistin concentration governs the bulk particle properties. As discussed earlier, such porous particles are produced as a consequence of colistin shell formation during droplet drying. The spray-dried meropenem showed poor aerosolization performance; while, the spray-dried colistin showed superior aerosolization performance, which was attributed to its low-cohesive propensity. Co-spraying with colistin improved the FPF of meropenem; Colistin-Meropenem_1:1 and Colistin-Meropenem_3:1 showed more than two-fold higher FPF compared with the spray-dried meropenem alone. This suggests that colistin exerts an aerosolization-enhancing effect. Morphologically, co-sprayed formulations appeared similar to spray-dried meropenem; however, porosity increased with an increase in colistin concentration. Porous particles with low density have lower aerodynamic diameters than those with the same geometric diameters but higher density, which lead to better aerosolization performance of these colistin-containing composite formulations (Telko & Hickey, 2005).

It is interesting to note that some interactions between colistin and meropenem as demonstrated by the FT-IR data (Figure 5 and Table 4). The changes in spectra were very significant for the formulation at the mass ratio of colistin to meropenem 1:1. In particular, the most notable change in spectra is that the O-H stretching band of the carboxyl group in meropenem shifted to the lower wavenumber. This kind of hydrogen bond is called red-shifting hydrogen bond which may be attributed to the lengthening and weakening of O-H bond due to its attraction to hydrogen acceptor. At the same time, the amide I C=O band of colistin is shifted to the higher wavenumber. From these spectral changes, it can be suggested that there is a hydrogen bond between the carboxyl O-H group of meropenem as a hydrogen donor and C=O groups of colistin as a hydrogen acceptor. This hypothesis can be supported by the fact that the amide II N-H bending was shifted to the higher wavenumber with a decreased intensity, which can be observed when the N-H is not involved in an interaction with hydrogen acceptor, but other group bonded to N, such as carbonyl, is involved in hydrogen bond as an acceptor. This is called blue shifted bond (Joseph & Jemmis, 2007). In addition, there were also significant band shifts of meropenem not only in the C–H wagging and twisting vibrations in the hydroxyethyl substituent and the β-lactam ring, but also in C-N stretching vibration in the pyrrolidine ring and dimethylcarbamoyl group, which indicate the change of overall structural conformation due to the forming of hydrogen bonding as reported previously (Paczkowska et al., 2016). All those changes in FTIR spectra could be an evidence for explanation of the intermolecular interactions *via* hydrogen bonding between meropenem and colistin. Furthermore, FTIR result accompanied with the results of XPS and aerosolization performance suggest that the uniform distribution of colistin at the surface of co-spray dried particles, which likely led to the aerosolization-enhancing effect.

Conclusions

In the present study, we developed and characterized co-spray dried colistin and meropenem DPI formulations which showed superior antibacterial activity. Incorporation of colistin improved the aerosolization performance of meropenem as evidenced by an almost two-fold increase in FPF, attributable to the enrichment of colistin on the particle surface and the increased porosity. FT-IR spectra demonstrated intermolecular interactions between colistin and meropenem. Such synergistic antimicrobial activities and increased aerosolization performance will not only improve the patient compliance by reducing the inhaled powder mass and minimizing local adverse effects, but also have potential to achieve superior therapeutic efficacy, which deserve further *in-vivo* studies using our established animal lung infection model (Y.-W. Lin et al., 2017; Y.-W. Lin et al., 2018).

Acknowledgments

Research reported in this publication was supported by the National Institute of Allergy and Infectious Diseases of the National Institutes of Health under Award Number R01AI132681. Jian Li and Tony Velkov are supported by a research grant from the National Institute of Allergy and Infectious Diseases of the National Institutes of Health (R01 AI111965). The content is solely the responsibility of the authors and does not necessarily represent the official views of the National Institutes of Health. Qi (Tony) Zhou is partially supported by the Ralph W. and Grace M. Showalter Research Trust Award. Jian Li is an Australian NHMRC Senior Research Fellow. The authors are grateful for the scientific and technical assistance of the Australian Microscopy & Microanalysis Research Facility at the Future Industries Institute, University of South Australia. The authors are thankful for access to FT-IR in Tonglei Li's lab. Kind donations of RS01 DPI device from Plastiape S.p.A. and HPMC capsules from Qualicaps, Inc. are acknowledged.

References

Abdelkader A, El-Mokhtar MA, Abdelkader O, Hamad MA, Elsabahy M, El-Gazayerly ON. Ultrahigh antibacterial efficacy of meropenem-loaded chitosan nanoparticles in a septic animal model. Carbohydrate polymers. 2017; 174:1041–1050. [PubMed: 28821026]

Biswas S, Brunel JM, Dubus JC, Reynaud-Gaubert M, Rolain JM. Colistin: an update on the antibiotic of the 21st century. Expert Review of Anti-Infective Therapy. 2012; 10(8):917–934. DOI: 10.1586/eri.12.78 [PubMed: 23030331]

Cai Y, Chai D, Wang R, Liang B, Bai N. Colistin resistance of Acinetobacter baumannii: clinical reports, mechanisms and antimicrobial strategies. Journal of Antimicrobial Chemotherapy. 2012; 67(7):1607–1615. DOI: 10.1093/jac/dks084 [PubMed: 22441575]

Chew NY, Chan HK. The role of particle properties in pharmaceutical powder inhalation formulations. Journal of Aerosol Medicine. 2002; 15(3):325–330. DOI: 10.1089/089426802760292672 [PubMed: 12396421]

Chew NY, Shekunov BY, Tong HH, Chow AH, Savage C, Wu J, Chan HK. Effect of amino acids on the dispersion of disodium cromoglycate powders. Journal of Pharmaceutical Sciences. 2005; 94(10):2289–2300. [PubMed: 16136546]

Chew NYK, Chan HK. Use of solid corrugated particles to enhance powder aerosol performance. Pharm Res. 2001; 18(11):1570–1577. DOI: 10.1023/a:1013082531394 [PubMed: 11758765]

Chew NYK, Tang P, Chan HK, Raper JA. How much particle surface corrugation is sufficient to improve aerosol performance of powders? Pharmaceutical Research. 2005; 22(1):148–152. [PubMed: 15771241]

Choi S-J, Lee B-G, YOON H-K, Park S-W, JUN S-A, Lee K-H, LIM B-J. 2012

Cielecka-Piontek J, Paczkowska M, Lewandowska K, Barszcz B, Zalewski P, Garbacki P. Solid-state stability study of meropenem – solutions based on spectrophotometric analysis. Chemistry Central Journal. 2013; 7:98–98. DOI: 10.1186/1752-153X-7-98 [PubMed: 23759021]

Cipolla D, Chan HK. Inhaled antibiotics to treat lung infection. Pharmaceutical Patent Analyst. 2013; 2(5):647–663. DOI: 10.4155/ppa.13.47 [PubMed: 24237172]

Davies TA, Shang W, Bush K, Flamm RK. Affinity of Doripenem and Comparators to Penicillin-Binding Proteins in Escherichia coli and Pseudomonas aeruginosa. Antimicrobial Agents and Chemotherapy. 2008; 52(4):1510–1512. DOI: 10.1128/aac.01529-07 [PubMed: 18250190]

de Boer AH, Chan HK, Price R. A critical view on lactose-based drug formulation and device studies for dry powder inhalation: Which are relevant and what interactions to expect? Advanced Drug Delivery Reviews. 2012; 64(3):257–274. DOI: 10.1016/j.addr.2011.04.004 [PubMed: 21565232]

Edwards DA, Caponetti G, Hrkach JS, Lotan N, Hanes J, Ben-Jebria A, Langer RS. Aerodynamically light particles for pulmonary drug delivery. Google Patents. 2005

Feng AL, Boraey MA, Gwin MA, Finlay PR, Kuehl PJ, Vehring R. Mechanistic models facilitate efficient development of leucine containing microparticles for pulmonary drug delivery. International Journal of Pharmaceutics. 2011; 409(1–2):156–163. DOI: 10.1016/j.ijpharm.2011.02.049 [PubMed: 21356284]

Freudenthal O, Quilès F, Francius G, Wojszko K, Gorczyca M, Korchowiec B, Rogalska E. Nanoscale investigation of the interaction of colistin with model phospholipid membranes by Langmuir technique, and combined infrared and force spectroscopies. Biochimica et Biophysica Acta (BBA)-Biomembranes. 2016; 1858(11):2592–2602. [PubMed: 27480806]

Garonzik SM, Li J, Thamlikitkul V, Paterson DL, Shoham S, Jacob J, … Nation RL. Population Pharmacokinetics of Colistin Methanesulfonate and Formed Colistin in Critically Ill Patients from a Multicenter Study Provide Dosing Suggestions for Various Categories of Patients. Antimicrobial Agents and Chemotherapy. 2011; 55(7):3284–3294. DOI: 10.1128/aac.01733-10 [PubMed: 21555763]

Grasmeijer F, Lexmond AJ, van den Noort M, Hagedoorn P, Hickey AJ, Frijlink HW, de Boer AH. New mechanisms to explain the effects of added lactose fines on the dispersion performance of adhesive mixtures for inhalation. PloS One. 2014; 9(1):e87825.doi: 10.1371/journal.pone.0087825 [PubMed: 24489969]

Herrmann G, Freitag E, Deppisch C, Heyder S, Graepler-Mainka U, Riethmüller J. Inhalative meropenem–tobramycin–colistin combination improves lung function in chronic Pseudomonas aeruginosa colonization. Journal of Cystic Fibrosis. 14:S86.

Jong T, Li J, Morton DA, Zhou QT, Larson I. Investigation of the Changes in Aerosolization Behavior Between the Jet-Milled and Spray-Dried Colistin Powders Through Surface Energy Characterization. Journal of Pharmaceutical Sciences. 2016; 105(3):1156–1163. DOI: 10.1016/s0022-3549(15)00189-6 [PubMed: 26886330]

Joseph J, Jemmis ED. Red-, blue-, or no-shift in hydrogen bonds: a unified explanation. Journal of the American Chemical Society. 2007; 129(15):4620–4632. [PubMed: 17375920]

Kitzis MD, Acar JF, Gutmann L. Antibacterial activity of meropenem against Gram-negative bacteria with a permeability defect and against staphylococci. Journal of Antimicrobial Chemotherapy. 1989; 24(suppl_A):125–132. DOI: 10.1093/jac/24.suppl_A.125 [PubMed: 2808204]

Lawrence S, Alpar H, McAllister S, Brown M. Liposomal (MLV) Polymyxin B: Physicochemical Characterization and Effect of Surface Charge on Drug Association. Journal of Drug Targeting. 1993; 1(4):303–310. DOI: 10.3109/10611869308996088 [PubMed: 8069572]

Lenhard JR, Bulitta JB, Connell TD, King-Lyons N, Landersdorfer CB, Cheah SE, … Holden PN. High-intensity meropenem combinations with polymyxin B: new strategies to overcome carbapenem resistance in Acinetobacter baumannii. Journal of Antimicrobial Chemotherapy. 2016; 72(1):153–165. [PubMed: 27634916]

Levin AS, Barone AA, Penço J, Santos MV, Marinho IS, Arruda EAG, … Costa SF. Intravenous colistin as therapy for nosocomial infections caused by multidrug-resistant Pseudomonas aeruginosa and Acinetobacter baumannii. Clinical Infectious Diseases. 1999; 28(5):1008–1011. [PubMed: 10452626]

Liang W, Liu X-f, Huang J, Zhu D-m, Li J, Zhang J. Activities of colistin-and minocycline-based combinations against extensive drug resistant Acinetobacter baumannii isolates from intensive care unit patients. BMC infectious diseases. 2011; 11(1):109. [PubMed: 21521536]

Lin YW, Zhou QT, Cheah SE, Zhao J, Chen K, Wang J, … Li J. Pharmacokinetics/pharmacodynamics of pulmonary delivery of colistin against Pseudomonas aeruginosa in a mouse lung infection model. Antimicrobial agents and chemotherapy. 2017; 61(3):e02025–02016. [PubMed: 28031207]

Lin YW, Zhou QT, Han ML, Chen K, Onufrak NJ, Wang J, … Chan H-K. Elucidating the Pharmacokinetics/Pharmacodynamics of Aerosolized Colistin against Multidrug-Resistant Acinetobacter baumannii and Klebsiella pneumoniae in a Mouse Lung Infection Model. Antimicrobial agents and chemotherapy. 2018; 62(2):e01790–01717. [PubMed: 29229637]

Lin YW, Wong J, Qu L, Chan HK, Zhou QT. Powder production and particle engineering for dry powder inhaler formulations. Current Pharmaceutical Design. 2015; 21(27):3902–3916. [PubMed: 26290193]

Mangal S, Meiser F, Tan G, Gengenbach T, Denman J, Rowles MR, … Morton DAV. Relationship between surface concentration of L-leucine and bulk powder properties in spray dried formulations. European Journal of Pharmaceutics and Biopharmaceutics. 2015; 94:160–169. DOI: 10.1016/j.ejpb.2015.04.035 [PubMed: 26007290]

Mangal S, Meiser F, Tan G, Gengenbach T, Morton DAV, Larson I. Applying surface energy derived cohesive–adhesive balance model in predicting the mixing, flow and compaction behaviour of interactive mixtures. European Journal of Pharmaceutics and Biopharmaceutics. 2016; 104:110–116. DOI: 10.1016/j.ejpb.2016.04.021 [PubMed: 27132984]

Mangal S, Nie H, Xu R, Guo R, Cavallaro A, Zemlyanov D, Zhou Q. Physico-Chemical Properties, Aerosolization and Dissolution of Co-Spray Dried Azithromycin Particles with L-Leucine for Inhalation. Pharmaceutical research. 2018; 35(2):28.doi: 10.1007/s11095-017-2334-9 [PubMed: 29374368]

Marchaim D, Chopra T, Pogue JM, Perez F, Hujer AM, Rudin S, … Kaye KS. Outbreak of Colistin-Resistant, Carbapenem-Resistant Klebsiella pneumoniae in Metropolitan Detroit, Michigan. Antimicrobial Agents and Chemotherapy. 2011; 55(2):593–599. DOI: 10.1128/aac.01020-10 [PubMed: 21115786]

Mestres C, Alsina MA, Busquets MA, Murányi I, Reig F. Interaction of colistin with lipids in liposomes and monolayers. International Journal of Pharmaceutics. 1998; 160(1):99–107. DOI: 10.1016/S0378-5173(97)00301-3

Mizgerd JP. Lung infection--a public health priority. PLoS Medicine. 2006; 3(2):e76.doi: 10.1371/journal.pmed.0030076 [PubMed: 16401173]

Momin MA, Tucker IG, Doyle CS, Denman JA, Das SC. Manipulation of spray-drying conditions to develop dry powder particles with surfaces enriched in hydrophobic material to achieve high aerosolization of a hygroscopic drug. International journal of pharmaceutics. 2018

Momin MA, Tucker IG, Doyle CS, Denman JA, Sinha S, Das SC. Co-spray drying of hygroscopic kanamycin with the hydrophobic drug rifampicin to improve the aerosolization of kanamycin powder for treating respiratory infections. International journal of pharmaceutics. 2018; 541(1–2):26–36. [PubMed: 29458207]

Montgomery AB, Vallance S, Abuan T, Tservistas M, Davies A. A randomized double-blind placebo-controlled dose-escalation phase 1 study of aerosolized amikacin and fosfomycin delivered via the PARI investigational eFlow(R) inline nebulizer system in mechanically ventilated patients. Journal of Aerosol Medicine and Pulmonary Drug Delivery. 2014; 27(6):441–448. DOI: 10.1089/jamp.2013.1100 [PubMed: 24383962]

Mouton JW. Combination therapy as a tool to prevent emergence of bacterial resistance. Infection. 1999; 27(2):S24–S28. DOI: 10.1007/bf02561666

Paczkowska M, Mizera M, Szymanowska-Powałowska D, Lewandowska K, Błaszczak W, Gościańska J, … Cielecka-Piontek J. β-Cyclodextrin complexation as an effective drug delivery system for meropenem. European Journal of Pharmaceutics and Biopharmaceutics. 2016; 99:24–34. [PubMed: 26592156]

Paterson DL, Harris PNA. Colistin resistance: a major breach in our last line of defence. The Lancet Infectious Diseases. 2016; 16(2):132–133. DOI: 10.1016/S1473-3099(15)00463-6 [PubMed: 26603171]

Rabbani NR, Seville PC. The influence of formulation components on the aerosolisation properties of spray-dried powders. Journal of Controlled Release. 2005; 110(1):130–140. DOI: 10.1016/j.jconrel.2005.09.004 [PubMed: 16226334]

Shekunov BY, Chattopadhyay P, Tong HHY, Chow AHL. Particle Size Analysis in Pharmaceutics: Principles, Methods and Applications. Pharmaceutical Research. 2007; 24(2):203–227. DOI: 10.1007/s11095-006-9146-7 [PubMed: 17191094]

Shetty N, Zeng L, Mangal S, Nie H, Rowles MR, Guo R, … Zhou Q. Effects of Moisture-Induced Crystallization on the Aerosol Performance of Spray Dried Amorphous Ciprofloxacin Powder Formulations. Pharmaceutical Research. 2018; 35(1):7.doi: 10.1007/s11095-017-2281-5 [PubMed: 29294198]

Singh A, Van den Mooter G. Spray drying formulation of amorphous solid dispersions. Advanced Drug Delivery Reviews. 2016; 100:27–50. DOI: 10.1016/j.addr.2015.12.010 [PubMed: 26705850]

Smyth HD, Hickey AJ. Carriers in drug powder delivery. American Journal of Drug Delivery. 2005; 3(2):117–132.

Sou T, Kaminskas LM, Nguyen TH, Carlberg R, McIntosh MP, Morton DA. The effect of amino acid excipients on morphology and solid-state properties of multi-component spray-dried formulations for pulmonary delivery of biomacromolecules. European Journal of Pharmaceutics and Biopharmaceutics. 2013; 83(2):234–243. [PubMed: 23183447]

Telko M, Hickey A. Dry powder inhaler formulation. Respiratory Care. 2005; 50(9):1209–1227. [PubMed: 16122404]

Timurkaynak F, Can F, Azap ÖK, Demirbilek M, Arslan H, Karaman SÖ. In vitro activities of non-traditional antimicrobials alone or in combination against multidrug-resistant strains of Pseudomonas aeruginosa and Acinetobacter baumannii isolated from intensive care units. International Journal of Antimicrobial Agents. 2006; 27(3):224–228. DOI: 10.1016/j.ijantimicag.2005.10.012 [PubMed: 16464562]

Traini D, Young PM. Delivery of antibiotics to the respiratory tract: an update. Expert Opinion on Drug Delivery. 2009; 6(9):897–905. DOI: 10.1517/17425240903110710 [PubMed: 19637984]

Vehring R. Pharmaceutical particle engineering via spray drying. Pharmaceutical Research. 2008; 25(5):999–1022. DOI: 10.1007/s11095-007-9475-1 [PubMed: 18040761]

Vehring R, Foss WR, Lechuga-Ballesteros D. Particle formation in spray drying. Journal of Aerosol Science. 2007; 38(7):728–746. DOI: 10.1016/j.jaerosci.2007.04.005

Velkov T, Abdul Rahim N, Zhou Q, Chan HK, Li J. Inhaled anti-infective chemotherapy for respiratory tract infections: Successes, challenges and the road ahead. Advanced Drug Delivery Reviews. 2015; 85:65–82. DOI: 10.1016/j.addr.2014.11.004 [PubMed: 25446140]

Velkov T, Deris ZZ, Huang JX, Azad MAK, Butler M, Sivanesan S, … Li J. Surface changes and polymyxin interactions with a resistant strain of Klebsiella pneumoniae. Innate Immunity. 2013; 20(4):350–363. DOI: 10.1177/1753425913493337 [PubMed: 23887184]

Wallace SJ, Li J, Nation RL, Prankerd RJ, Velkov T, Boyd BJ. Self-assembly behavior of colistin and its prodrug colistin methanesulfonate: implications for solution stability and solubilization. The Journal of Physical Chemistry B. 2010; 114(14):4836–4840. [PubMed: 20302384]

Wan F, Bohr A, Maltesen MJ, Bjerregaard S, Foged C, Rantanen J, Yang M. Critical Solvent Properties Affecting the Particle Formation Process and Characteristics of Celecoxib-Loaded PLGA Microparticles via Spray-Drying. Pharmaceutical Research. 2013; 30(4):1065–1076. DOI: 10.1007/s11095-012-0943-x [PubMed: 23263784]

Weers J. Inhaled antimicrobial therapy - barriers to effective treatment. Adv Drug Deliv Rev. 2015; 85:24–43. DOI: 10.1016/j.addr.2014.08.013 [PubMed: 25193067]

WHO. The 10 leading causes of death in the world, 2000 and 2012. May, 2014. who.int/mediacentre/factsheets/fs310/en/

Yapa SWS, Li J, Porter CJH, Nation RL, Patel K, McIntosh MP. Population pharmacokinetics of colistin methanesulfonate in rats: Achieving sustained lung concentrations of colistin for targeting respiratory infections. Antimicrobial Agents and Chemotherapy. 2013; 57(10):5087–5095. DOI: 10.1128/AAC.01127-13 [PubMed: 23917323]

Zhou Q, Denman JA, Gengenbach T, Das S, Qu L, Zhang H, … Morton DAV. Characterization of the surface properties of a model pharmaceutical fine powder modified with a pharmaceutical lubricant to improve flow via a mechanical dry coating approach. Journal of Pharmaceutical Sciences. 2011; 100(8):3421–3430. DOI: 10.1002/jps.22547 [PubMed: 21455980]

Zhou Q, Gengenbach T, Denman JA, Yu HH, Li J, Chan HK. Synergistic Antibiotic Combination Powders of Colistin and Rifampicin Provide High Aerosolization Efficiency and Moisture Protection. Aaps j. 2014; 16(1):37–47. DOI: 10.1208/s12248-013-9537-8 [PubMed: 24129586]

Zhou Q, Leung SSY, Tang P, Parumasivam T, Loh ZH, Chan HK. Inhaled formulations and pulmonary drug delivery systems for respiratory infections. Advanced Drug Delivery Reviews. 2015; 85:83–99. DOI: 10.1016/j.addr.2014.10.022 [PubMed: 25451137]

Zhou Q, Morton DAV, Yu HH, Jacob J, Wang J, Li J, Chan HK. Colistin Powders with High Aerosolisation Efficiency for Respiratory Infection: Preparation and In Vitro Evaluation. Journal of Pharmaceutical Sciences. 2013; 102(10):3736–3747. DOI: 10.1002/jps.23685 [PubMed: 23904207]

Zhou QT, Loh ZH, Yu J, Sun SP, Gengenbach T, Denman JA, … Chan HK. How Much Surface Coating of Hydrophobic Azithromycin Is Sufficient to Prevent Moisture-Induced Decrease in Aerosolisation of Hygroscopic Amorphous Colistin Powder? Aaps j. 2016; 18(5):1213–1224. DOI: 10.1208/s12248-016-9934-x [PubMed: 27255350]

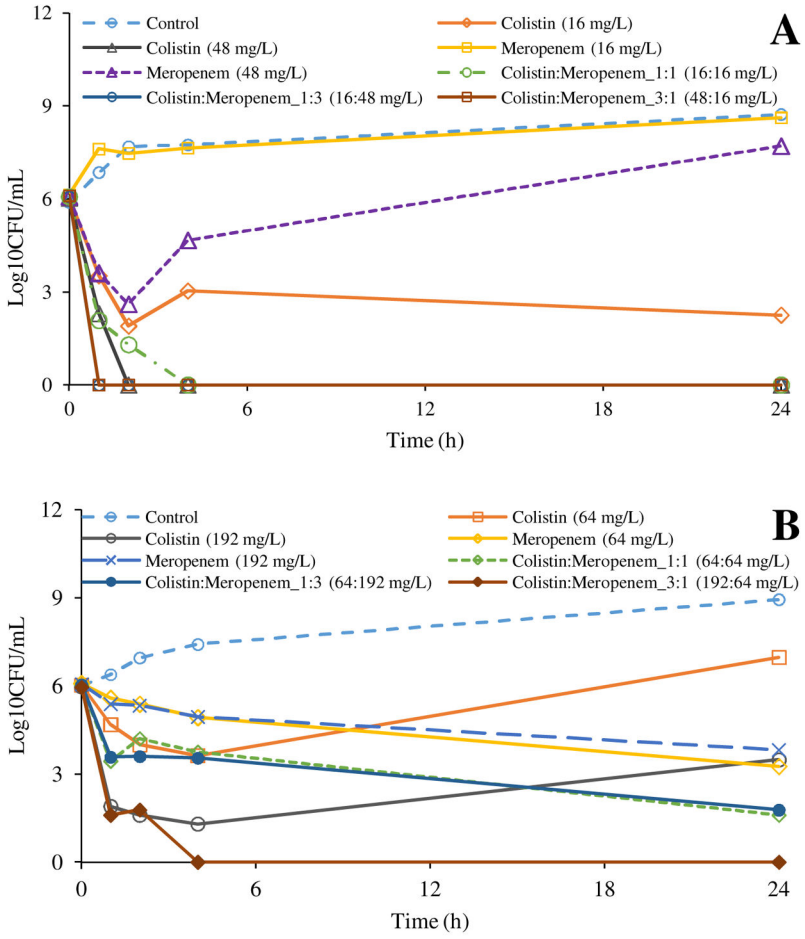

Figure 1.

Time-kill kinetics of colistin, meropenem and their combinations against *A. baumannii* N16870 (A) *and P. aeruginosa* 19147 (B).

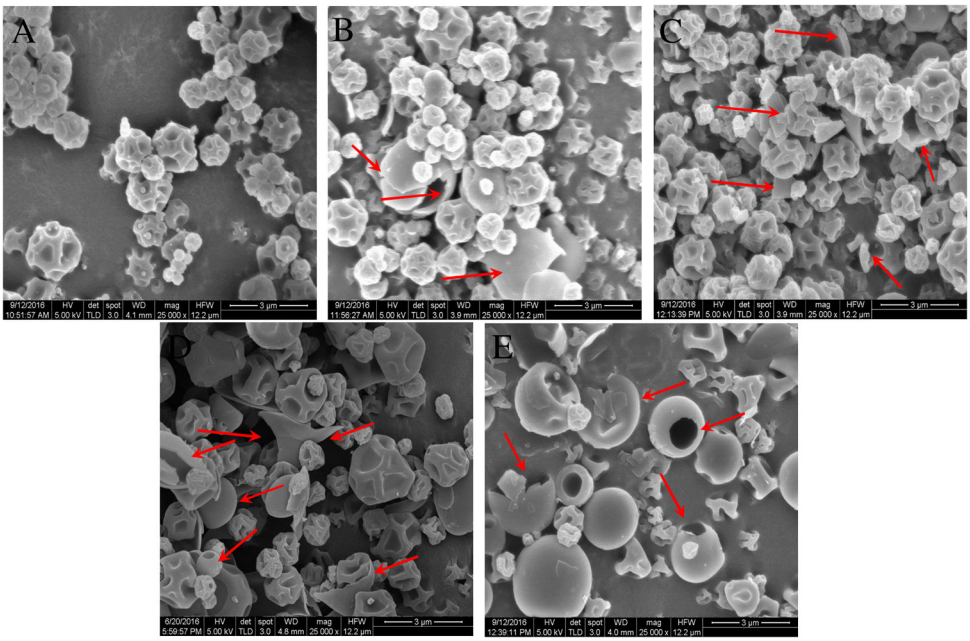

Figure 2.

Representative scanning electron microscopy images of: (A) Meropenem-SD; (B) Colistin:Meropenem_1:3; (C) Colistin:Meropenem_1:1; (D) Colistin:Meropenem_3:1; and (E) Colistin-SD. Red arrows point out smooth particles (hollow or flake).

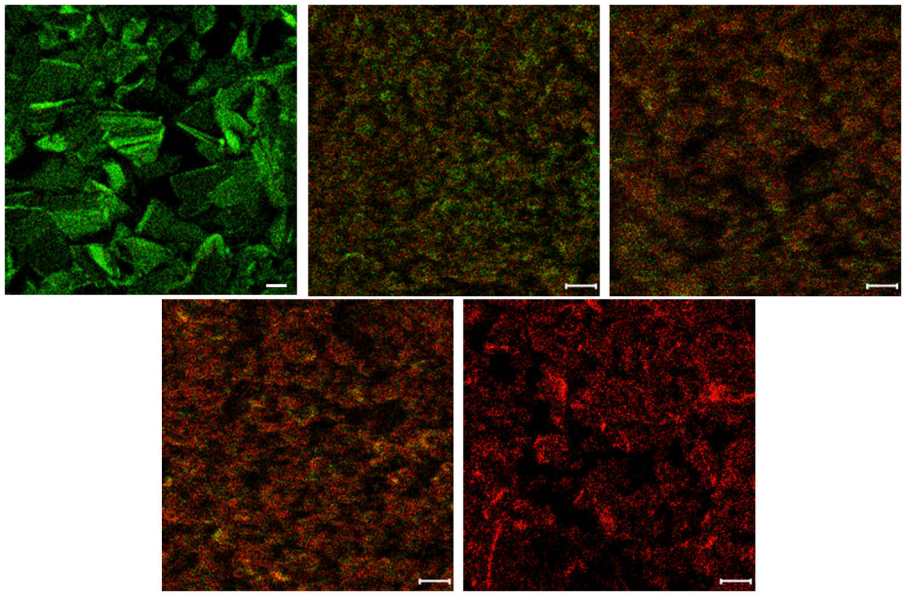

Figure 3.

Surface composition distributions of colistin (red) and meropenem (green) on the surfaces of composite particles obtained by ToF-SIMS. A-Raw Meropenem; B-Colistin:Meropenem_1:3; C- Colistin:Meropenem_1:1; D- Colistin:Meropenem_3:1 and E-Raw Colistin (scale bar represents 10 μm).

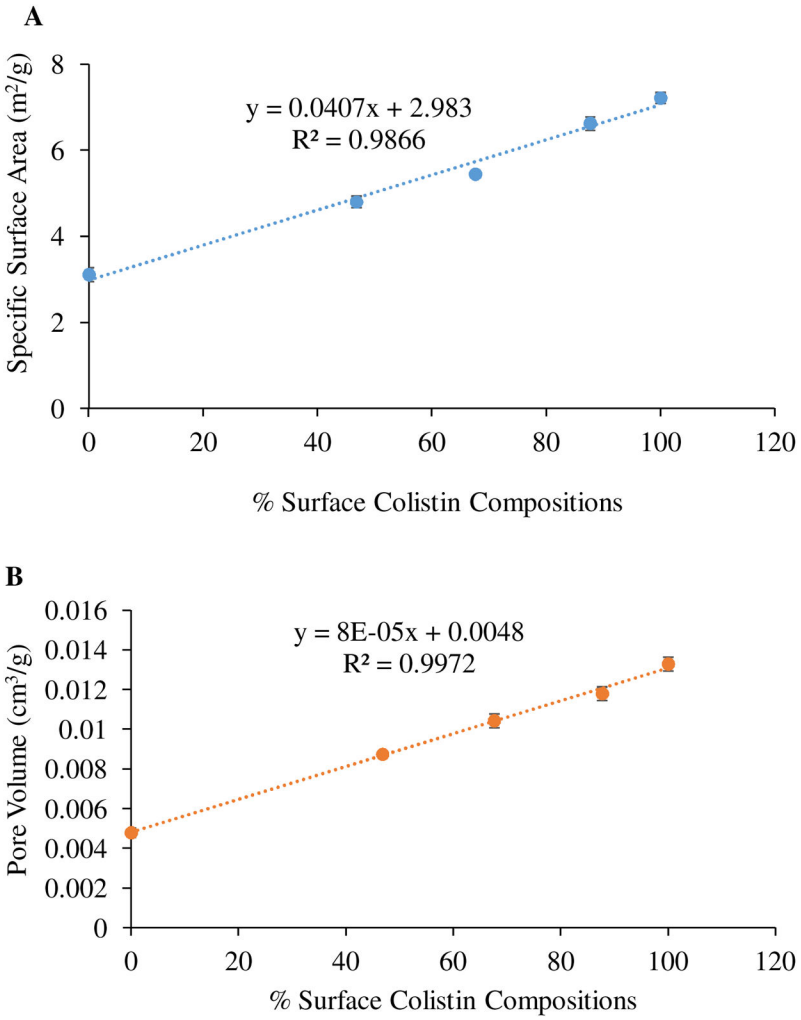

Figure 4.

Specific surface area (A) and pore volume (B) of spray-dried formulations as a function of % surface colistin composition.

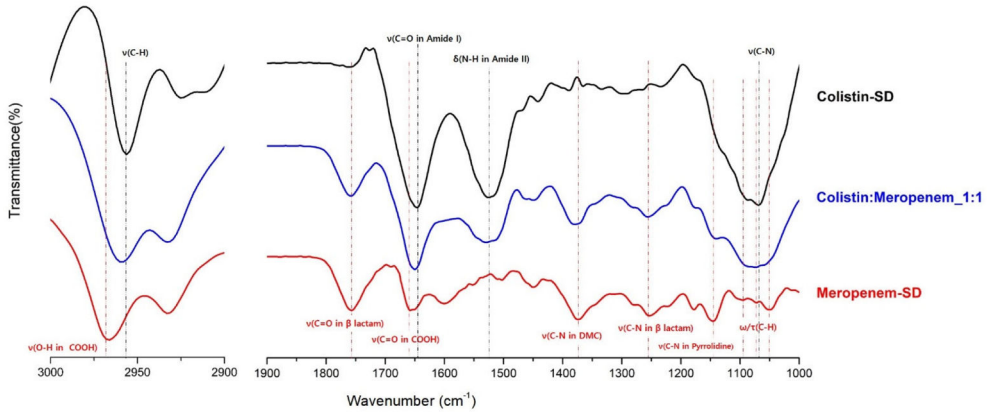

Figure 5.

FTIR spectra of various spray-dried formulations (ν: stretching, δ: bending, τ: twisting, ω: wagging, DMC: dimethylcarbamoyl)

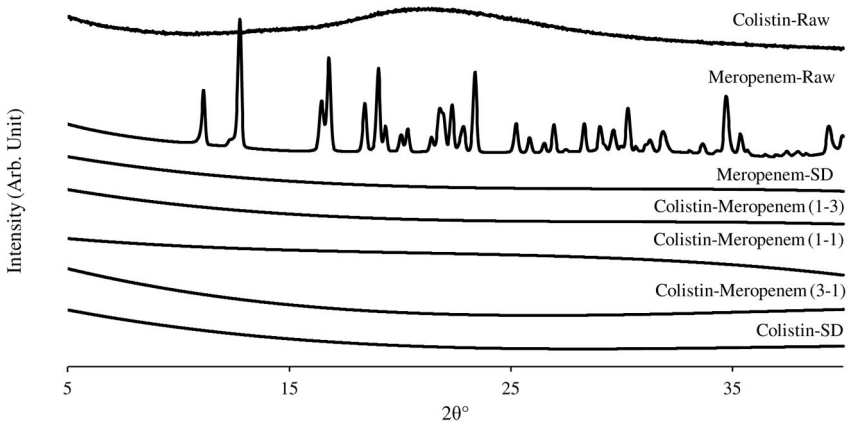

Figure 6.
X-ray diffraction patterns of the raw materials and the spray-dried powder formulations

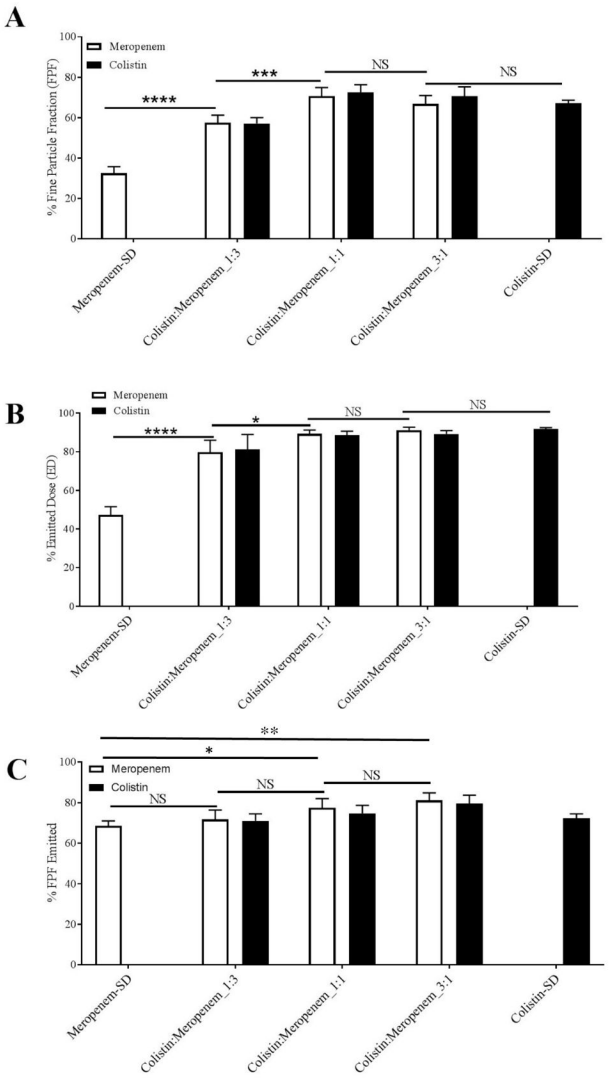

Figure 7.

In-vitro aerosol performance of: (A) fine particle fraction (% FPF); (B) emitted dose (% ED); FPF-Emitted (% FPF-Emitted) of the spray-dried formulations. The data are presented as mean ± SD (n=4).

Table 1

Particle sizes of the spray-dried powder formulations.

Formulation	Particle Size (μm)		
	D_{10}	D_{50}	D_{90}
Meropenem-SD	0.8 ± 0.1	1.1 ± 0.1	1.9 ± 0.3
Colistin-Meropenem_1:3	1.0 ± 0.2	1.4 ± 0.1	2.1 ± 0.3
Colistin-Meropenem_1:1	1.0 ± 0.1	1.2 ± 0.1	1.5 ± 0.4
Colistin-Meropenem_3:1	0.8 ± 0.1	1.2 ± 0.1	1.7 ± 0.1
Colistin-SD	1.0 ± 0.2	1.5 ± 0.1	2.7 ± 0.3

Table 2

Specific surface area and pore volume of the spray-dried formulations. The data are presented as mean ± SD (n = 3).

Formulation	Specific surface area (m^2/g)	Pore volume (cm^3/g)
Meropenem-SD	3.1 ± 0.2	0.005 ± 0.001
Colistin:Meropenem_1:3	4.8 ± 0.1	0.009 ± 0.001
Colistin:Meropenem_1:1	5.4 ± 0.1	0.010 ± 0.001
Colistin:Meropenem_3:1	6.6 ± 0.2	0.012 ± 0.001
Colistin-SD	7.2 ± 0.1	0.013 ± 0.001

Table 3

Molar composition of colistin and meropenem on the surfaces of composite formulations based on theoretical calculation and XPS measurement.

Formulation	% Theoretical Composition		% Measured Surface Composition	
	Colistin	Meropenem	Colistin	Meropenem
Colistin:Meropenem_1:3	26.0	74.0	46.8	53.2
Colistin:Meropenem_1:1	51.4	48.6	67.6	32.4
Colistin:Meropenem_3:1	76.0	24.0	87.7	12.3

Table 4

FTIR band assignment of various spray-dried formulations

Band assignment		Wavenumber (cm^{-1})		
		Colistin	**Colistin: Meropenem_1:1**	**Meropenem**
Colistin	C-H stretching	2956.3		NA
	Amide I C=O stretching	1645.0	1650.8	
	Amide II N-H bending	1525.4	1531.2	
	C-N stretching	1068.4	1074.1	
Meropenem	Carboxyl O-H stretching	NA	2958.2	
	β-lactam C=O stretching		1758.7	1756.8
	Carboxyl C=O stretching		1650.8	1658.5
	Dimethylcarbamoyl C-N stretching		1380.8	1373.1
	β-lactam C-N stretching		1255.4	1253.5
	Pyrrolidine C-N stretching		1139.7 1074.1	1145.5
				1095.4
				1072.2
	Hydroxyethyl and β-lactam C-H wagging and twisting		1074.1	1051.0